Applied Surface Science 257 (2011) 6821–6828

Applied Surface Science

journal homepage: www.elsevier.com/locate/apsusc

Photocatalytic performance of silver TiO_2: Role of electronic energy levels

L. Gomathi Devi*, K. Mohan Reddy

Department of Chemistry, Central College, Bangalore University, Dr. BR Ambedkar Veedi, Bangalore 560001, India

ARTICLE INFO

Article history:
Received 2 December 2010
Received in revised form 1 March 2011
Accepted 1 March 2011
Available online 8 March 2011

Keywords:
Silver metallized TiO_2
Degussa P25
Inter band transition
Congo Red
Sol–gel TiO_2

ABSTRACT

Nano-sized silver deposits on the surface of Degussa P25 TiO_2 (Ag-DP25) particles act as sites of electron accumulation where the reduction of adsorbed species takes place. Electrons can be transferred from Degussa P25 TiO_2 (DP25) to Ag particles because of the difference in the work functions of the two materials. The efficiency of the electron transfer depends on the size and the distribution of metal deposits. A significant photocatalytic oxidation enhancement by metal deposit will only be observed if the metal deposits play a more dominant role than just increasing the life time of charge carriers. The properties of metal deposits like, loaded amount, oxidation state of the deposit and its size will influence the performance. Further, a decrease in band-gap in DP25 and Ag-DP25 was observed due to the carbide ion substitution for the oxide ion in TiO_2. Such unintentional carbon incorporation is expected mostly in combustion synthesized materials. Silver metal deposits and unintentional incorporation of the carbon shows the beneficial effect by specific mechanism in the photocatalytic degradation of Congo Red (CR).

1. Introduction

The degradation of the dissolved organic compounds in water using photocatalysis has attracted much attention because it is easy to handle, inexpensive, stable and effective [1–10]. Among the various metal oxide semiconductors, TiO_2 has received prime importance due to its chemical stability and adoptable electronic and optical property [2–5,11,12]. Titanium dioxide is the most extensively studied photocatalytic material, with outstanding physical and chemical properties. On excitation, electrons are promoted to the conduction band and holes are consequently generated in its valence band. Such charge carriers are able to reduce and oxidize many species adsorbed on the semiconductor particles and induces the oxidative destruction of organics up to their mineralization [3–11]. However, its high band gap and high rate of electron–hole recombination limits its efficiency in photocatalytic reactions [13,14]. Both these limitations can be overcome by the metallization of TiO_2 photocatalytic particles. Noble metal modified semiconductors have high Schottky barriers acting as electron traps promoting interfacial electron transfer, thereby suppressing the recombination [15–19]. Metal islands deposited on the semiconductor surface have been shown to efficiently trap the electron and the free hole in the valence band can successively participate in the oxidation reactions [20]. The equilibration of the Fermi-level between the metal and the semiconductor favours electron accumulation in the composite metal/TiO_2 system. The deposition of Ag nanoparticles on the Degussa P25 titanium dioxide (DP25) surface is explained in the present study as a means of improving its photocatalytic activity in the degradation of CR in the aqueous phase under UV irradiation. The effect of pH on the photocatalytic activity of metallized semiconductor particles is explored. Under UV light irradiation, the photogenerated electrons quickly transfer from TiO_2 surface to the Ag particles, leading to the effective separation of electron–hole and results in the improvement of photocatalytic efficiency. It has been reported in the literature that the noble metals such as Pt [21,22], Ag, and Au [2,23] deposited on TiO_2 have the high Schottky barriers among the metals and thus acts as electron traps, facilitating electron–hole separation and promotes the interfacial electron transfer process [24,25]. Though wide research studies are available in the literature on the photocatalytic destruction of various organic and inorganic pollutants, the studies on silver deposited TiO_2 photocatalyst involving various energy levels are still limited in the literature [26–28]. The present study aims to understand the governing factors leading to the efficiency of silver metallized TiO_2 particles in a photocatalytic reaction. In this regard commercially available Degussa P25 (DP25) sample is silver metallized by photo reduction method (Ag-DP25). The model compound chosen for the study is Congo Red (CR) an azo dye which is highly soluble in water and persists for long time once discharged to the environment. The effects of deposition of Ag species on the surface states, surface Plasmon effect and the various energy levels created within the bandgap are the subject matter of discussion.

* Corresponding author. Tel.: +91 80 22961336; fax: +91 80 22961331.
E-mail address: gomatidevi_naik@yahoo.co.in (L. Gomathi Devi).

0169-4332/$ – see front matter © 2011 Elsevier B.V. All rights reserved.
doi:10.1016/j.apsusc.2011.03.006

2. Experimental

2.1. Chemicals

Commercially available Degussa P25 (surface area is 55 m^2/g) was used as starting material to prepare silver metallized Ag-DP25. Silver nitrate ($AgNO_3$), oxalic acid ($C_2H_2O_4$), hydrogen peroxide (H_2O_2) and Congo Red (CR) were obtained from Aldrich chemicals. Sodium hydroxide (NaOH), hydrochloric acid (HCl), ammonium per sulphate ($(NH_4)_2S_2O_8$) (APS) and potassium per sulphate ($K_2S_2O_8$) (KPS) were supplied from SD Fine Chemicals. The CR has the molecular formula $C_{32}H_{22}N_6O_6S_2Na_2$ and the corresponding molecular weight is 697, shows λ_{max} at 497 nm. CR shows deep blue colour in acid medium and changes to red colour under alkaline condition due to the resonance effects.

2.2. Preparation of Ag-DP25 and sol–gel-TiO_2

Ag-DP25 photocatalyst is prepared based on the reduction of $AgNO_3$ in the presence of oxalic acid on DP25 in a suspension as prepared by Szabo-Bardos et al. [15,16]. Metallic silver is deposited on DP25 (Ag-DP25) surface by photodeposition method. An aqueous solution of $AgNO_3$ (2×10^{-4} M), oxalic acid (5×10^{-3} M) with DP25 (1 g) was added to 1 l of distilled water and it is stirred vigorously. The pH of the suspension was adjusted to 6.8–7.0 by the addition of 0.1 N NaOH solution and the suspension is irradiated with UV-light for 40–50 min. After the irradiation the solution containing Ag–TiO_2 was then allowed to stand for 6 h. The colour of the reaction mixture was observed to change from white to violet-brown under UV light, indicating the reduction of Ag^+ to Ag^0 and deposition of Ag^0 on DP25. Hermann and Sclafani have proposed a mechanism describing the deposition and growth of silver particles on the titania surface [21]. Silver ions are initially adsorbed on the surface of TiO_2 particles. Photogenerated electrons reduce adsorbed Ag^+ ions to silver metal atoms. The formation of small crystallites of silver can occur either by the agglomeration of silver atoms or by a cathodic like successive reduction process. The agglomeration of silver atoms can be described in the following way:

$$TiO_2(e^-, h^+) + Ag^+_{adsorbed} \rightarrow TiO_2Ag^0(h^+)$$

The successive reduction sequence is represented by

$$mAg^0 \rightarrow Ag_m$$

The brown solid is filtered, dried and was heated to 120 °C for 2 h in an incubation to evaporate water and the colour of the solid catalyst changes to pale pink which confirms the deposition [29]. The absence of silver in the aliquot sample of reaction mixture confirms the deposition of noble metal on the semiconductor particles. From the above process the obtained deposition of Ag was 0.23 wt%. The concentration of $AgNO_3$ and oxalic acid is changed with respect to the percentage of deposition accordingly. The concentration of $AgNO_3$ is $(0.4347, 0.8696, 5.2174, 8.6954, 17.3913) \times 10^{-4}$ M for 0.05, 0.1, 0.6, 1.0, 2.0 wt% of Ag respectively. The preparation of sol–gel TiO_2 (SG-TiO_2) is as mentioned in previous study [30].

2.3. Analytical techniques

Powdered X-ray diffraction (PXRD) patterns were recorded using Bruker aXs Model D8 Advanced powder X-ray diffractometer with a Cu Kα source (λ = 1.541 Å) and the scanning range employed was $2\theta = 5–85°$ at a scan rate of 2°/min. The average crystallite size was calculated using the Scherrer's formula. The X-ray diffraction line broadening was obtained with a slow scanning speed of 1/2°/min. The particle size is obtained by scanning electron microscopy (SEM) analysis of the samples using JEOL-JSM-6490 LV scanning electron microscopy. The energy dispersive X-ray microanalysis (EDX) was done using Oxford INCA 250 energy dispersive X-ray micro analyzer. The absorption and diffuse reflectance spectra were recorded (with $BaSO_4$ as reference) by using double beam UV-3101 PC UV–VIS–NIR Shimadzu spectrophotometer. The spectra were recorded at room temperature in the range of 200–800 nm. FTIR spectra were recorded using FTIR-840 OS Shimadzu FTIR spectrophotometer in the frequency range 4000–400 cm^{-1} using KBr as the standard reflectance sample. X-ray photoelectron spectra (XPS) were recorded with ESCA-3 Mark II spectrometer (VG Scientific Ltd., UK) using Al Kα radiation (1486.6 eV).

2.4. Photocatalysis procedure

The degradation reaction mixture consists of 250 ml of 10 ppm aqueous CR solution along with 40 mg of the photocatalyst (DP25/Ag-DP25). The initial pH of the CR aqueous suspension was found to be 6.6. The pH variation during the course of reaction was not significant, so all the runs were carried out at natural pH conditions of 6.6. In the experiments with oxidizing agent, the optimized amount 40 mg of the catalyst is added to the reaction mixture in the beginning of the experiments. The reaction mixture was stirred vigorously using magnetic stirrer for the entire time span of the experiment. The initial decrease in the concentration of CR in the dark will give the extent of adsorption on the catalyst particles. 3 ml of sample solution was periodically withdrawn from the reactor and analyzed after removal of catalyst particles by centrifugation at 3000 rpm for 15 min. The UV-lamp consists of medium pressure mercury vapour lamp with a photon flux of 7.75 mW/cm^2 whose wavelength is around 350–400 nm.

3. Results and discussion

3.1. Characterization of photocatalysts DP25 and Ag-DP25

3.1.1. Powder X-ray diffraction (PXRD)

Fig. 1 shows PXRD patterns of DP-25 and Ag-DP25. The PXRD pattern shows mainly anatase with minor rutile in the ratio of 80:20. The major peaks at $2\theta = 25.3°$ for (1 0 1) of anatase and $2\theta = 27.4°$ of (1 1 0) of rutile is observed in all the samples. Silver peak in PXRD is noticed only for the sample 1.0 wt% Ag-DP25 at $2\theta = 44.3°$ for (3 3 1). Very low concentration of Ag is undetectable from PXRD technique. Further at high concentration of silver an additional peak of diminished intensity at 32.5° corresponding to Ag_2O of (2 2 0) is also observed. If the metal is not reduced completely during the photodeposition, the possibility of formation of Ag_2O cannot be ruled out, but this is observed only at higher concentrations of silver. The anatase: rutile lattice structure of DP25 is unperturbed and silver deposition did not affect the phase struc-

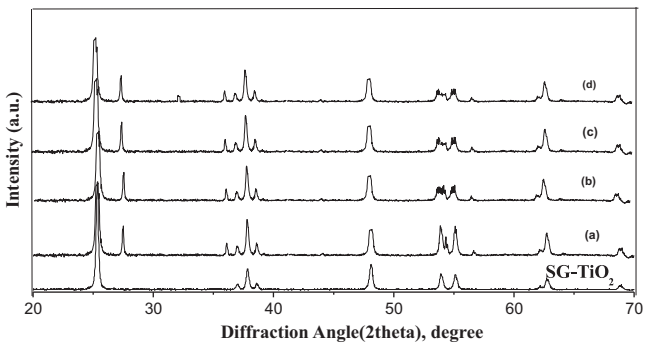

Fig. 1. PXRD patterns of the SG-TiO_2, (a) DP25, (b) 0.05 wt% Ag-DP25, (c) 0.1 wt% Ag-DP25 and (d) 0.6 wt% Ag-DP25 samples.

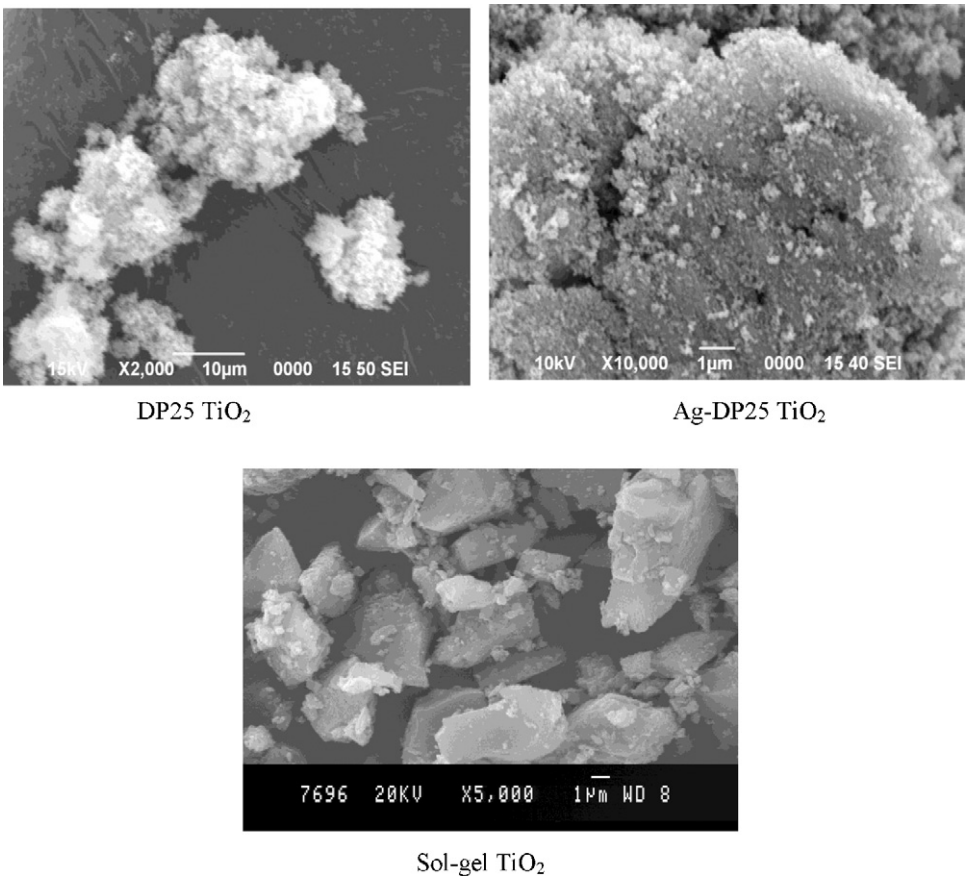

Fig. 2. SEM images of DP25, Ag-DP25 (0.6 wt%), sol–gel TiO_2.

ture of DP25. The sol–gel TiO_2 shows only anatase phase (JCPDS, No. 21-1272) as shown in Fig. 1.

3.1.2. SEM and EDX

In order to investigate the morphology of the synthesized photocatalyst particles, SEM and EDX analysis were carried out. Fig. 2 shows SEM images of DP25, Ag-DP25 and SG-TiO_2. The SEM images show that silver particles are of the range of 5 nm and are homogeneously distributed on TiO_2 grains. SEM picture indicates better dispersion with very less agglomeration. The image illustrate that Ag-DP25 particles have spherical and smooth surface due to the deposition silver.

EDX results show the perfect matching of atom percentage composition of DP25, Ag-DP25 and SG-TiO_2. Qualitative determination was done by using grid supported carbon film of 15–25 nm thickness which gives exceptionally low background. The atomic % and weight % values are represented in Table 1. The fractional percentage of carbon detected was neglected in this study since the grid supported carbon film was used.

3.1.3. UV–visible absorption and diffuse reflectance spectra (UV–vis)

UV–visible absorption spectra were recorded to investigate the optical absorption properties of catalysts in the range of 200–800 nm as shown in Fig. 3a and 3b. It can be observed that DP25 and SG-TiO_2 had no absorption in the visible region (>400 nm). Ag-DP25 had significant absorption between 400 and 600 nm. The strong Plasmon resonance absorption at wavelength above 400 nm is due to the Ag nanoparticles deposits on DP25 surface. Light absorption by the deposited metal causes a collective oscillation of the free conduction band electrons of the silver nanoparticles as a consequence of their optical excitation. This phenomenon is observed when the wavelength of the incident light far exceeds the particle diameter. The absorption between 400 and 800 nm increases with increase in Ag content (the spectra shown in the figure contains only 0.6 wt% of Ag). The diffuse reflectance spectra show λ_{max} at 388, 370, 377.1 nm for SG-TiO_2, DP25, and Ag-DP25 0.6 wt% respectively which corresponds to the band gap of 3.2, 3.351, 3.288 eV.

Table 1
EDX data of DP25, Ag-DP25 and sol–gel TiO_2.

Photocatalyst	Element	Weight%		Atom%	
		Observed	Approximate value	Observed	Approximate value
DP25	Ti	52.02	52	23.15	23
	O	47.96	48	76.85	77
Ag-DP25	Ti	40.85	41	22.49	22
	O	45.95	46	75.92	76
	Ag	13.20	13	1.49	1
Sol–gel TiO_2	Ti	58.23	58	30.42	30
	O	41.77	42	69.58	70

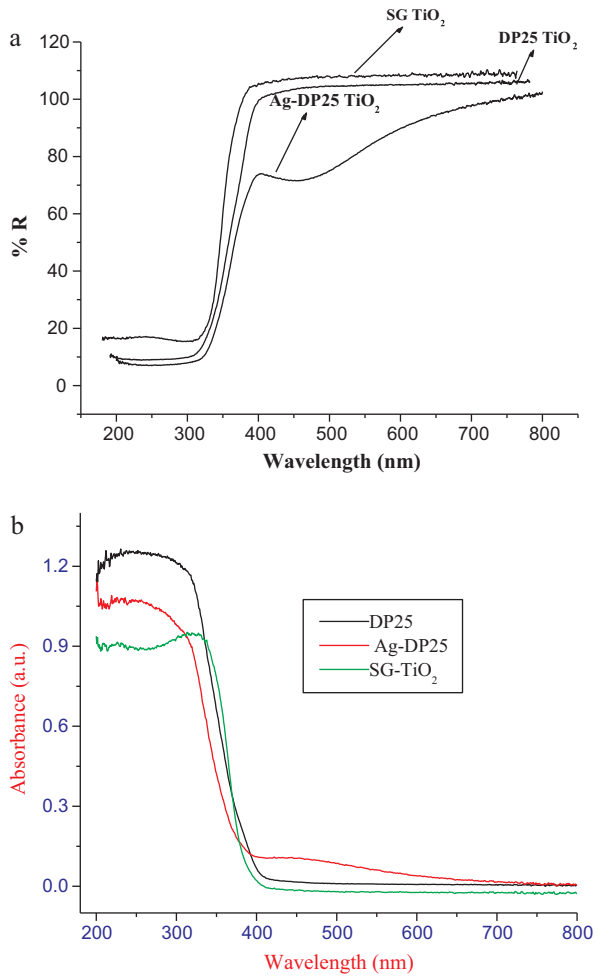

Fig. 3. (a) UV–visible reflectance spectra of SG-TiO_2, DP25 TiO_2 and Ag-DP25 TiO_2 (0.6 wt%) catalysts. (b) UV–visible absorption spectra of SG-TiO2, DP25 and Ag-DP25 (0.6 wt%) catalysts.

3.1.4. Infrared spectra

The infrared spectra of SG-TiO_2, DP25 and Ag-DP25 sample in the range of 4000–400 cm^{-1} show a broad band at 3400 cm^{-1} which can be assigned to the O–H stretching vibration of Ti–OH. The other narrow band ~1637 cm^{-1} can be assigned to O–H bending mode of hydroxyl group or to the stretching mode of Ti–O which could be the envelope of the bonds of Ti–O–Ti bond of titanium oxide network. Further, DP25 and Ag-DP25 samples showed a prominent narrow band ~1107 cm^{-1} which could be attributed to the C–O stretching vibration. But this band is not observed in SG-TiO_2.

3.1.5. BET isotherms

BET isotherms were recorded for all the samples to obtain the surface area and pore size volumes. DP25 has the highest surface area of 55 m^2/g and the surface area decreased to 48 m^2/g after silverization. Therefore, the metallized surface area should be around 7 m^2/g. SG-TiO_2 shows the lowest surface area of 20 m^2/g as presented in Table 2. DP25 shows highest pore volume and pore diameter and this decrease with silver metallization is due to the coverage of pores by silver metal deposits.

3.1.6. XPS analysis

The chemical state and the composition of Ag deposit on DP25 surface and near surface region were studied by XPS as shown in Fig. 4a–c. The Ag $3d_{5/2}$ peak appeared at a binding energy of 367.169 eV and for $3d_{3/2}$ at 373.1 eV with a peak separation of 5.931 eV and these values correspond to metallic silver [31]. The Ti binding energies were observed at 458.43 eV and 464.196 eV which can be assigned to Ti $2p_{3/2}$ and Ti $2p_{1/2}$ with a peak separation of 5.739 eV which can be assigned to Ti^{4+} in TiO_2. The O_{1s} peaks were observed at 529.668 eV. The surface atomic concentration of O 1s is 72.7 and 70.5%, Ti 2p is 27.3 and 24.2%, Ag 3d is 0.0 and 5.3% in TiO_2 and Ag-DP25 respectively. Surprisingly, though there was no carbon incorporation either by doping or by any other means, the XPS carbon 1s binding energy at 285.71 eV was observed in both DP-25 and Ag-DP25 samples, whereas no such peak was obtained in SG-TiO_2. These results substantiated the results obtained from the IR spectral analysis (where C–O bond stretching vibration was observed at 1107 cm^{-1}). Such unintentional incorporation of the carbon as substituent can be expected especially in combustion synthesized TiO_2 [27]. This peak at 285.71 eV can be assigned to graphitic carbon [1,27,28]. This confirms the possible substitution of C in the form of $TiO_{2-x}C_x(Vo)_x$, where $(Vo)_x$ is the x number of vacant oxygen sites created for charge neutralization.

3.2. Photocatalytic activity

The degradation of CR was tested for the various catalysts with different compositions of silver content on DP25 TiO_2 (0.05, 0.1, 0.6 and 1.0 wt% of Ag) and it was observed that the degradation of CR was most efficient for 0.6 wt% Ag-DP25 catalyst, as shown in Fig. 5. Tables 3 and 4 show the results of comparison of the catalytic activity of DP25, Ag-DP25 and SG-TiO_2. As observed the catalytic activity of Ag-DP25 shows enhanced activity compared with reference catalyst DP25. The extent of increase in the rate constant from DP25 to Ag-DP25 is around 1.5 times and that of SG-TiO_2 to DP25 the observed increase in the rate constant is 1.3 times. The activity of SG-TiO_2 seems to be lowest and the increase in the rate constant is 1.8 times compared to Ag-DP25. The effect of pH on the degradation of CR can be analyzed by the data in Table 2 irrespective of the catalyst used, the rate of degradation seems to be high at pH 6.6, though the extent of degradation vary with the catalyst even at this pH. At pH 6.6 the catalyst surface may be slightly positively charged or it is almost neutral due to its isoelectric point. The surface active sites on catalyst surface should either behave as Lewis acid sites of medium acidity or it should be completely neutral. This state of catalyst should be highly favourable for the adsorption of CR molecule. This may be due to the stearic hindrance arising from the presence of fused aromatic rings consisting of naphthalene and biphenyl moieties which may resist its adsorption at other pH conditions. Table 3 shows the results of a comparison of catalytic activity of Ag-DP25, DP25 and SG-TiO_2. Experimentally it was observed that the catalytic activity of the deposited catalyst increased with the increase in Ag content due to the higher charge separation efficiency. But when the weight of Ag exceeded above 0.6 wt% a decrease in activity was observed. Especially for >1.0 wt% of Ag, the activity decreases

Table 2
BET data of DP-25 Ag-deposited TiO_2 and sol–gel TiO_2 samples.

Catalyst	Density (g/cc)	BET area (m^2/g)	Pore volume (cc/g)	Pore diameter (Å)
DP-25	3.7676	55	0.08121	49.654
Ag-TiO_2	3.8912	48	0.05948	49.437
Sol–gel TiO_2	3.9412	20	0.01564	56.902

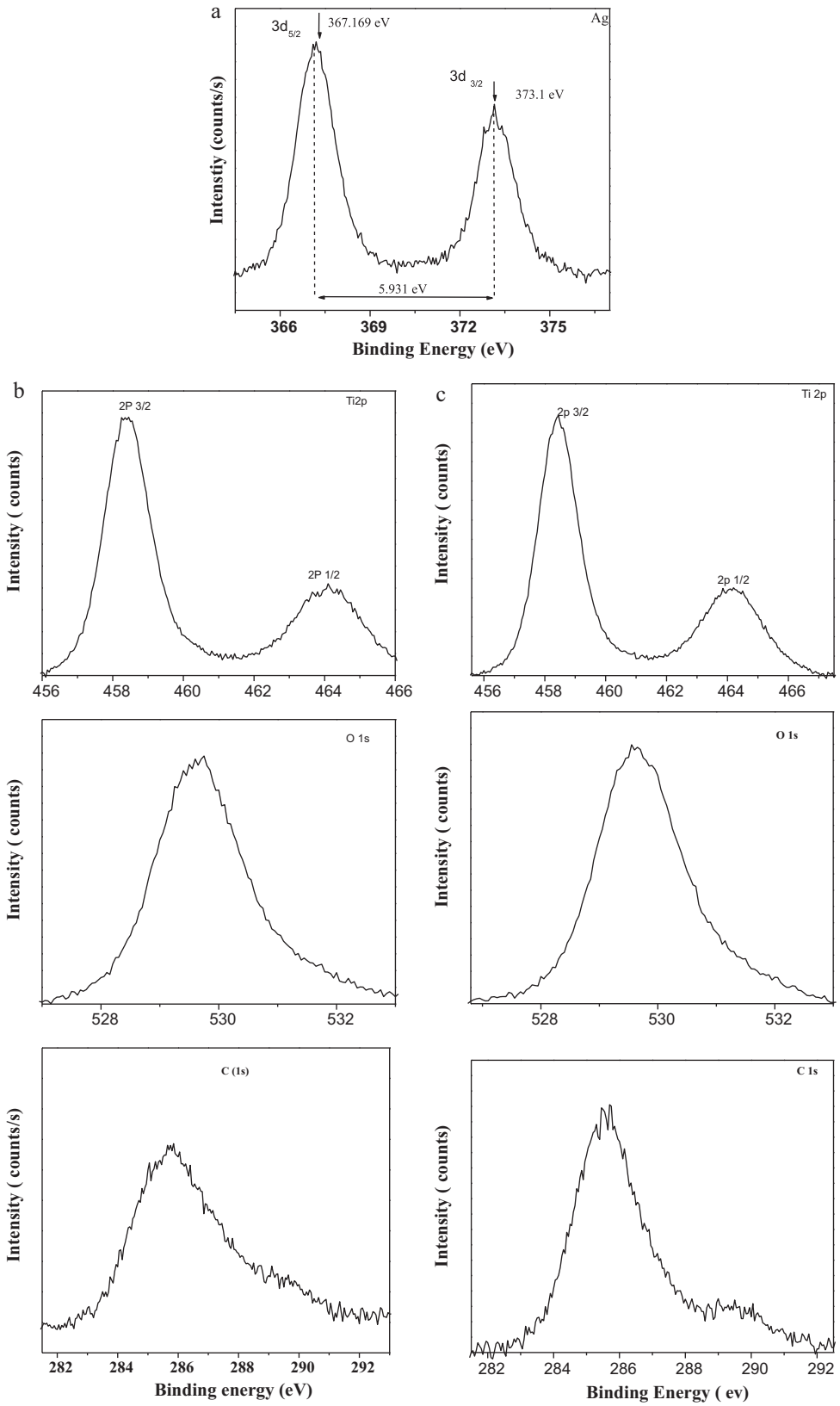

Fig. 4. (a) The Ag 3d region of the XPS spectrum of the Ag–TiO_2 layer. (b) The Ti 2p, O 1s and C 1s region of the XPS spectrum of the Ag–TiO_2 layer. (c) The Ti 2p, O 1s and C 1s region of the XPS spectrum of the TiO_2 layer.

to such an extent that the catalyst shows lesser activity than the SG-TiO_2. Higher Ag content becomes detrimental as the surface of the catalyst gets covered and bare surface to absorb the photons decreases by blocking the light reaching the surface. Above the optimum level the Ag deposits act as recombination centres due to the negatively charged silver sites may begin to attract positively charge holes. The other possible reason could be a decrease in the electron density in TiO_2 lattice due to the excess electron attraction

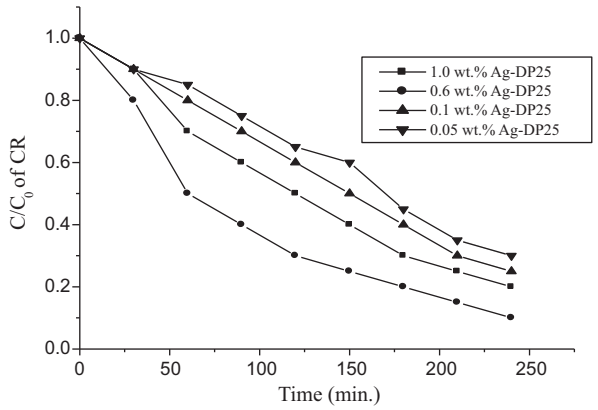

Fig. 5. Photocatalytic degradation of the CR using various catalysts 1.0 wt% Ag-DP25, 0.6 wt% Ag-DP25, 0.1 wt% Ag-DP25 and 0.05 wt% Ag-DP25.

Table 3
Effect of pH on the degradation of CR (for the time interval of 240 min).

Photocatalyst	pH	% degradation
Ag-DP25	3.0	40
	6.6	95
	9.0	42
DP25	3.0	30
	6.6	80
	9.0	31
Sol–gel TiO_2	3.0	25
	6.6	62
	9.0	28

by the numerous metal deposits formed at higher concentrations which may result in field configuration and can show detrimental effect on the charge separation.

3.3. Comparison of photocatalytic activities of different titania samples

The observed photocatalytic activities among the catalysts Ag-DP25, DP25 and SG-TiO_2 can be analyzed in the following way: photocatalytic activity of the catalysts shows the following order Ag-DP25 > DP25 > SG-TiO_2 (Fig. 6). The observed enhancement in the case of Ag-DP25 is due to the metallization, in spite of having large comparable surface areas. In addition to the metallization Ag-DP25 and DP25 had shown that these samples had incorporated carbon in the lattice. The two possible ways of incorporation can be as a cation replacing Ti, or as an anion substituting O. The possibility of the second option being more, since incorporation of C has taken place spontaneously during the process of preparation of the catalyst. Carbon as a tetravalent ion may not influence the position of valence band and conduction band, instead it can induce an inter band gap vacant electronic state which can be expected to be located above valence band at 1.08 eV [1]. This carbon may act as an effective adsorbant to concentrate the pollutant molecules around the TiO_2 particles [32]. The adsorbed pollutant seemed to be supplied to the silver loaded TiO_2 mostly by surface diffusion. In this way the carbon can possibly indirectly prevent

Table 4
Pseudo-first order rate constant and the corresponding regression coefficient for the photodegradation of CR.

Photocatalyst	k (min^{-1})	R^2
Ag-DP25	7.425×10^{-2}	0.9925
DP25	5.254×10^{-2}	0.9641
TiO_2	4.2351×10^{-2}	0.9542

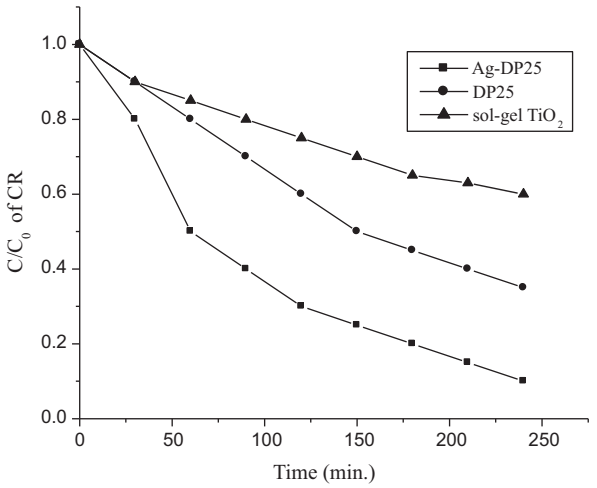

Fig. 6. Photocatalytic degradation of CR using three different catalysts TiO_2, DP25, Ag-DP25 (0.6 wt%).

recombination of electron–hole pairs. Metallization and incorporated carbon may show additional positive enhancement in the case of Ag-DP25. The presence of carbon in the case of DP25 is also beneficial, where as no such carbon could be noticed in the case SG-TiO_2.

3.4. Effect of oxidants on the degradation process

Fig. 7 shows the photocatalytic degradation experiments carried out in the presence of oxidizing agent alone (in absence of catalyst and UV light irradiation) which shows negligible degradation. Efficient degradation takes place in the presence of catalyst and oxidizing agent under UV light. The oxidizing agents used were H_2O_2, APS and KPS (10 ppm) which primarily acts as electron acceptors. They undergo photolysis to give hydroxyl and persulphate radicals. They inhibit the recombination of photogenerated electron–hole pairs thereby enhancing the degradation rate. The $OH^{\bullet}$ and $SO_4^{\bullet -}$ radicals formed during illumination are extremely potent oxidizing agents having the oxidation potential of 2.8 V and 2.6 V respectively. These radicals are involved in different reactions such as abstraction of hydrogen atom, adding to aromatic compounds and removing one electron from certain neutral molecules and they also acts as a trap for photogenerated electrons. The degradation

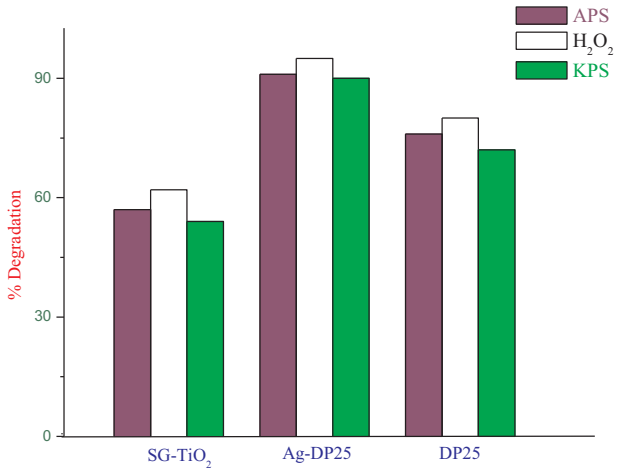

Fig. 7. Percentage degradation of the CR dye using different photocatalysts SG-TiO_2, DP25 TiO_2 and Ag-TiO_2 (0.6 wt%).

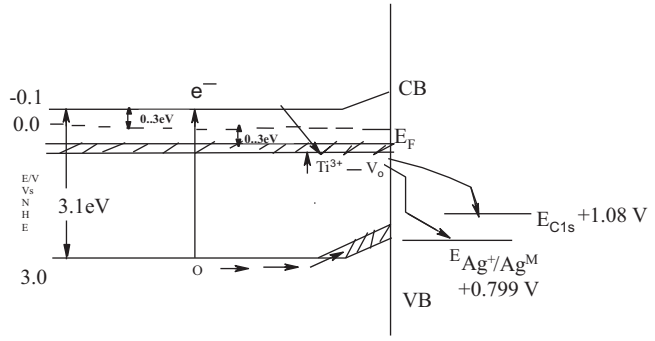

Fig. 8. Schematic energy level diagram for Ag-DP25 with energy levels of $E\ Ag^{+}/Ag^{M}$ and C_{1s} levels (the energy levels are drawn with respect to normal hydrogen electrode. The change in the potential at different pH conditions with respect to NHE is given by the equation: $V_{pzc} = 0.56 - 2.3(RT/F)$ pH, where V_{pzc} is the potential in Volts, R is the real gas constant, T is the temperature in K and F is the Faraday current in Coulombs).

rate is maximum for Ag-DP25 compared to DP25 and SG-TiO_2 and the comparison of these three oxidants shows that the difference between them is only marginal. This could be accounted to the pH of the solution. With the addition of H_2O_2, the pH of the solution is 6.7 and with APS the pH is 6.0. The pH of the reaction solution influences the band edge positions of the semiconductor and also the adsorption characteristics of pollutants since the pH change is favourable and comparable to the neutral pH (the solution as prepared) the difference between these three oxidants is marginal. The oxidation potential of H_2O_2 and APS is 1.78 V and 2.01 V respectively. There is 5–10% increase in the degradation rate in the presence of oxidants.

3.5. Schematic electronic energy levels of Ag-DP25

The energy levels of various electronic states can be located anywhere within the bandgap and allow inelastic capture of e^- or h^+s from the semiconductor bands. These states that are located nearer to the Fermi level can be filled with conduction band electron. In the present case the energy level nearer to Fermi level is Ti^{3+}–V_o state which has been created due to the presence of trace amounts of carbon (Fig. 8). The number of e^-s being transferred from the conduction band into these surface states [33] is given by:

$$dn_s/dt = \sigma_e V_e n_s (1-f) N_s$$

where f represents the electron occupation factor, σ_e is the cross section for electron capture at these surface states, V_e is the thermal velocity of the electrons, N_s is the density of the surface state and n_s the surface electron density. The defect state located 0.3 eV below E_F may arise from Ti^{3+}-V_o state. The photo excited e^-s from the conduction band can move downhill into the Ti^{3+}–V_o states from where they can move in to the either Ag metal deposits or to the C_{1s} states. In addition the C_{1s} state either can act as electron capturing centre or it can maximize the adsorption and to concentrate the pollutant molecules around Ag-DP25. The electrons trapped in the metallized silver are efficiently detrapped to the organic molecules for the efficient oxidation in Ag-DP25. Absence of such metal deposits in DP25 decreases the efficiency compared to Ag-DP25. However C_{1s} still facilitates the adsorption in DP25 and therefore shows higher efficiency than SG-TiO_2.

4. Conclusions

Photocatalytic degradation of CR using the DP25 and Ag-DP25 with various amounts of silver in metallic state was investigated. The result shows that metallized DP25 catalysts show enhancement in the degradation of CR when compared to that of pure DP25 at optimum silver loading. XPS studies have shown the incorporation of C_{1s} level in both DP25 and Ag-DP25. The involvement of this unintentionally incorporated carbon is explored. The activity of these catalysts is also studied in the presence of oxidizing agents like H_2O_2, APS and KPS. Silver metal deposits and unintentional incorporation of the carbon shows the beneficial effect by specific mechanism in the photocatalytic degradation of Congo Red (CR).

Acknowledgements

Financial assistance from Department of Science and Technology (DST) Major Research Project (2009-2012), Government of India is greatly acknowledged. The authors would like to thank Professor M.S. Hegde, Indian Institute of Science, Bangalore for helping in recording XPS analysis and Dr. Sarala Upadhya for SEM and EDX analysis.

References

[1] Shahed, U.M. Khan, M. Al-Shahry, W.B. Ingler Jr., Efficient photochemical water splitting by a chemically modified n-TiO_2, Science 297 (2002) 2243–2245.
[2] P.V. Kamat, Photochemistry on nonreactive and reactive (semiconductor) surfaces, Chem. Rev. 93 (1993) 267–300.
[3] M. Schiavello (Ed.), Photocatalysis and Environment Trends and Applications, Kluwer Academic Publishers, Dordrecht, 1988.
[4] E. Pelizzetti, N. Serpone (Eds.), Photocatalysis Fundamentals and Applications, Wiley, New York, 1989.
[5] M.R. Hoffmann, S.C. Martin, W. Choi, D.W. Behnemann, Environmental applications of semiconductor photocatalysis, Chem. Rev. 95 (1995) 69–96.
[6] W. Choi, A. Termin, M.R. Hoffmann, The role of metal-ion dopants in quantum-sized TiO_2: correlation between photoreactivity and charge carrier recombination dynamics, J. Phys. Chem. 98 (1994) 13669–13679.
[7] M. Anpo, Photocatalysis on titanium oxide catalysts: approaches in achieving highly efficient reactions and realizing the use of visible light, Catal. Surv. Jpn. 1 (1997) 169–179.
[8] A. Hogfelt, M. Gretzel, Light-induced redox reactions in nanocrystalline systems, Chem. Rev. 95 (1995) 49–68.
[9] J.M. Herrman, H. Tahiri, Y. Ait-Ichou, G. Lassaletta, A.R. Gonzalaz-Elipe, A. Fernandez, Characterization and photocatalytic activity in aqueous medium of TiO_2 and Ag–TiO_2 coatings on quartz, Appl. Catal. B: Environ. 13 (1997) 219–228.
[10] D.S. Ollis, H. Al-Ekabi, Photocatalytic Purification and Treatment of Water and Air, Elsevier, Amsterdam, 1993.
[11] Y. Ohko, I. Ando, C. Niwa, T. Tatsuma, T. Yamamura, T. Nakamura, Degradation of bisphenol-A in water by TiO_2 photocatalyst, Environ. Sci. Technol. 35 (2001) 2365–2369.
[12] J.M. Lee, M.S. Kim, B.W. Kim, Photodegradation of bisphenol-A with TiO_2 immobilized on the glass tubes including the UV light lamps, Water Res. 38 (2004) 3605–3613.
[13] T. Torimoto, Y. Okawa, N. Takeda, H. Yoneyama, Effect of activated carbon content in TiO_2-loaded activated carbon on photodegradation behaviors of dichloromethane, J. Photochem. Photobiol. A: Chem. 103 (1997) 153–157.
[14] R.K. Wahi, W.W. Yu, Y. Liu, M.L. Mejia, J.C. Falkner, Whitney Nolte, L. Vicki Colvin, Photodegradation of Congo Red catalyzed by nanosized TiO_2, J. Mol. Catal. A: Chem. 242 (2005) 48–56.
[15] E. Szabo-Bardos, H. Czili, A. Horvath, J. Photochem. Photobiol. A: Chem. 154 (2003) 195–201.
[16] E. Szabo-Bardos, H. Czili, A. Horvath, J. Photochem. Photobiol. A: Chem. 184 (2006) 221–227.
[17] W.D. Kingery, H.K. Bowen, D.R. Ulmann, Introduction to Ceramics, Wiley-Interscience, New York, 1976.
[18] A. Sarkany, Z. Revay, Appl. Catal. A: Gen. 243 (2003) 347–355.
[19] H.H. Kim, S.M. Oh, A. Ogata, S. Futamura, Appl. Catal. B: Environ. 56 (2005) 213–220.
[20] F.B. Li, X.Z. Li, Chemosphere 48 (2002) 1103–1111.
[21] J.M. Hermann, A. Sclafani, J. Photochem. Photobiol. A: Chem. 113 (1998) 181–188.
[22] A. Wold, Chem. Mater. 5 (1993) 280–283.
[23] C.Y. Wang, C.Y. Liu, X. Zheng, J. Chen, T. Shen, Colloids Surf. A: Chem. 131 (1998) 271–280.
[24] J.M. Hermann, J. Disdier, M.N. Mozzanega, P. Pichat, J. Catal. 60 (1979) 369–377.
[25] A. Henglein, J. Phys. Chem. 83 (1979) 2209–2216.
[26] V. Vamathevan, R. Amal, D. Beydoun, G. Low, S. McEvoy, J. Photochem. Photobiol. A: Chem. 148 (2002) 233–245.
[27] K. Nagaveni, G. Sivalingam, M.S. Hegde, G. Madras, Appl. Catal. B: Environ. 48 (2004) 83–93.

[28] G. Sivalingam, K. Nagaveni, M.S. Hegde, G. Madras, Appl. Catal. B: Environ. 45 (2003) 23–38.
[29] L. Gomathi Devi, K. Mohan Reddy, Appl. Surf. Sci. 256 (2010) 3116–3121.
[30] L. Gomathi Devi, G.M. Krishnaiah, J. Photochem. Photobiol. A: Chem. 121 (1999) 141–145.
[31] X. Zhang, M. Zhou, L. Lei, Mater. Chem. Phys. 91 (2005) 73–79.
[32] L. Amalric, C. Guillard, P. Pichat, J. Photochem. Photobiol. A: Chem. 52 (1995) 257–262.
[33] T.R.N. Kutty, L. Gomathi Devi, Ind. J. Technol. 24 (1986) 391–398.